X-ray standing wave investigation of submonolayer barium and strontium surface phases on Si(001)

D. M. Goodner,[1] D. L. Marasco,[2] A. A. Escuadro,[1] L. Cao,[1] and M. J. Bedzyk[1,3]
[1]*Department of Materials Science and Engineering and Materials Research Center, Northwestern University, Evanston, Illinois 60208, USA*
[2]*Department of Physics and Astronomy, Northwestern University, Evanston, Illinois 60208, USA*
[3]*Materials Science Division, Argonne National Laboratory, Argonne, Illinois 60439, USA*
(Received 28 November 2004; published 20 April 2005)

Submonolayer (2×1) Ba/Si(001) and (2×1) Sr/Si(001) surface phases have been studied with normal Si(004) and off-normal Si(022) x-ray standing wave (XSW) measurements. These results are compared to previous XSW measurements of a (2×3) phase of Sr on Si(001). The (004) and (022) coherent positions indicate that alkaline-earth metal (AEM) atoms occupy the same type of high symmetry site in the (2×1) Ba/Si(001), (2×1) Sr/Si(001), and (2×3) Sr/Si(001) surface phases. The difference between the AEM adatom heights measured for the (2×1) Ba/Si(001) and (2×1) Sr/Si(001) phases is consistent with the difference in the ionic radii of Ba and Sr. Consideration of the nearest neighbor AEM-Si bond lengths that would result from AEM atoms sitting on symmetrically dimerized Si(001) at the height specified by the Ba and Sr coherent positions strongly suggests that the AEM atoms occupy valley-bridge sites.

DOI: 10.1103/PhysRevB.71.165426 PACS number(s): 68.35.Bs, 68.43.Fg, 68.47.Fg, 68.49.Uv

I. INTRODUCTION

Ongoing efforts to find a high-K dielectric material to replace SiO_2 as the gate dielectric in field effect transistors (FETs) have generated significant interest in submonolayer phases of alkaline-earth metal (AEM) atoms on the Si(001) surface. $SrTiO_3$ is potentially useful as a gate dielectric in future FETs due to its relatively high dielectric constant and the small lattice mismatch ($\sim$1.7%) between the $SrTiO_3$(100) and Si(110) planes. $SrTiO_3$ films may also serve as effective buffer layers for the integration of other oxide materials with Si.[1,2] Cross-sectional transmission electron microscopy studies[3,4] have indicated that epitaxial $SrTiO_3$ films can be grown on Si(001) without forming unwanted secondary phases at the Sr–$SrTiO_3$ interface by preceding film growth with the formation of an ordered surface phase consisting of submonolayer amounts of Sr on the Si(001) substrate. Parallel interest in submonolayer phases of another AEM atom, Ba, on Si(001) has also risen due to the chemical and structural similarities between the Ba/Si(001) and Sr/Si(001) surfaces as well as some experimental evidence[5] that a Ba/Si(001) surface can be used as a template for growing $BaTiO_3$ on Si(001).

Submonolayer surface phases of Ba/Si(001) and Sr/Si(001) have been studied previously by low-energy electron diffraction (LEED),[6–12] Auger electron spectroscopy (AES),[8,11,12] reflection high energy electron diffraction (RHEED),[13] scanning tunneling microscopy (STM),[14–19] angle-integrated ultraviolet photoelectron spectroscopy (AIUPS),[20] ion scattering,[21] x-ray photoemission spectroscopy (XPS),[22] x-ray standing waves (XSW),[23,24] and density functional theory (DFT) calculations.[5,17,25–27] Most of the atomic-scale structural models proposed for the various short and long-range ordered AEM/Si(001) surface structures observed at AEM coverages between 0 and 1/2 ML consist of individual AEM adatoms occupying valley-bridge sites on a dimerized Si(001) surface. However, other models consisting of AEM dimers, AEM atoms occupying cave sites and individual AEM atoms substituted for Si dimers have also been proposed.[15,19,20]

A significant amount of atomic-scale structural information about the Sr/Si(001) surface has also been inferred from experimental and theoretical studies of $SrTiO_3$ films grown on Si(001) using a Sr/Si(001) surface reconstruction as a "template" layer for $SrTiO_3$ growth.[4,28–34] Various schemes for incorporating this layer into the $SrTiO_3$ film growth process have been described in Refs. 3, 13, and 35. Most of the recent reports of $SrTiO_3$ growth on Si(001) have described the use of a 1/2 ML (2×1) Sr/Si(001) template layer, although McKee *et al.*[3] reported the employment of a 1/4 ML $c(4\times2)$ Sr/Si(001) surface.

In the present work, we report on XSW measurements made on (2×1) phases of Ba/Si(001) and Sr/Si(001) surfaces using normal (004) and off-normal (022) Bragg reflections and compare these results to our previously reported XSW measurements of a (2×3) Sr/Si(001) surface phase.[24] The XSW results are used to triangulate the AEM atomic positions relative to the bulk primitive Si unit cell and indicate that AEM adatoms occupy the same type of site in the the (2×1) Ba/Si(001), (2×1) Sr/Si(001), and (2×3) Sr/Si(001) surface phases. Consideration of the possible AEM-Si bond lengths that would result from AEM atoms occupying the bulk primitive cell positions determined by XSW supports valley-bridge site occupancy, but plausible models with AEM atoms occupying other sites are also discussed.

II. EXPERIMENT

Experiments were conducted at the 12ID-D x-ray undulator BESSRC-CAT experimental station at the Advanced Pho-

ton Source, Argonne National Laboratory. Molecular beam epitaxy sample preparation, AES, LEED, and XSW measurements were performed in an ultrahigh vacuum (UHV) system with a base pressure $\sim 1.5 \times 10^{-10}$ Torr.

Single-crystal Si(001) samples were treated with a modified Shiraki etch[36] and mounted in a strain-free manner onto molybdenum sample-holders prior to introduction into the UHV system. After degassing ~ 12 h at 400–600 °C, samples were annealed for 15 min at 850–900 °C to remove the chemically grown SiO_2 film and produce a sharp, two-domain (2×1) LEED pattern indicating a dimerized Si(001) surface.

Effusion cells were used to deposit 0.7–1.0 ML (1 ML $= 6.78$ nm^{-2}, the areal number density of top-layer Si atoms on a bulk-terminated Si(001) surface) of AEM atoms onto the room-temperature Si(001) substrates. Subsequent anneals at 700–860 °C caused portions of the AEM atom coverage to desorb and resulted in sharp two-domain (2×1) LEED patterns. The extent of AEM atom desorption depended on both the time and temperature used during annealing. Two-domain (2×1) Sr/Si(001) surfaces were produced by annealing for 1–10 min at 700–750 °C, and two-domain (2×1) Ba/Si(001) surfaces were prepared by annealing for 1–5 min at 800–860 °C. The AEM atom coverage for both types of (2×1) surfaces ranged from 0.3 to 0.6 ML. The AEM coverage was determined in UHV by comparing the intensity of the Ba $L\alpha$ and Sr $K\alpha$ fluorescence signals from the samples to those of Ba and Sr-implanted Si standards calibrated by Rutherford backscattering spectroscopy (RBS). Sample temperature was monitored using an optical pyrometer and a thermocouple mounted on the sample stage.

UHV XSW measurements were conducted using an incident photon energy of 8.00 keV for the Ba/Si(001) surface and 18.46 keV for Sr/Si(001). The incident beam from the undulator was filtered by a high-heat-load Si(111) monochromator followed by a postmonochromator consisting of a pair of detuned nondispersive Si channel-cut crystals. The d spacing of the postmonochromator matched that of the sample. Samples were scanned in angle through the Si (004) and (022) Bragg conditions while monitoring the diffracted beam intensity with a photodiode and collecting the x-ray fluorescence spectra with a Si(Li) solid state detector. The Ba and Sr coherent fractions (f_H) and coherent positions (P_H) were determined by fitting the reflectivity and normalized Ba $L\alpha$ and Sr $K\alpha$ fluorescence yield data to dynamical diffraction theory. For more XSW experimental details, see Refs. 37 and 38.

III. RESULTS AND DISCUSSION

Figure 1 shows the experimental data from Si(004) and Si(022) XSW measurements of a two-domain (2×1) Ba/Si(001) surface with a coverage of 0.31(3) ML and a two-domain (2×1) Sr/Si(001) (2×1) surface with a coverage of 0.47(3) ML. Corresponding theoretical fits to the data, along with the f_H and P_H values determined from each XSW measurement are also shown in Fig. 1. Assuming the ordered AEM adatoms on a particular sample occupy only

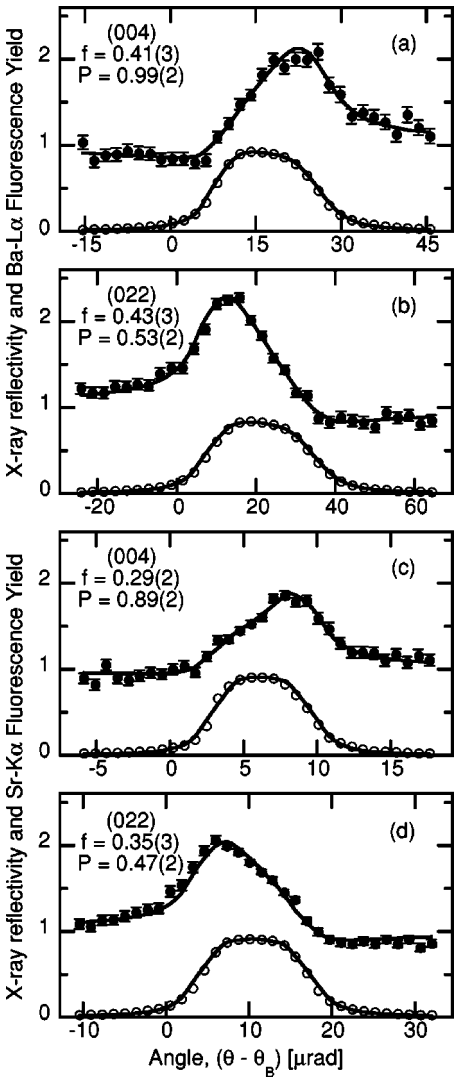

FIG. 1. Angular dependence of x-ray reflectivity (open circles) and fluorescence yield (filled circles) data (fit to dynamical diffraction theory) for (a) Si(004) and (b) Si(022) XSW measurements of a (2×1) Ba/Si(001) surface as well as (c) Si(004) and (d) Si(022) XSW measurements of a (2×1) Sr/Si(001) surface.

one type of site, the height, h, of these adatoms above the ideal bulk plane of second layer Si atoms is given by

$$h = (P_{004} + n)d_{004}\ \text{Å} \tag{1}$$

d_{004} is the Si(004) d spacing in Å, and n is an integer. Since the XSW is a periodic probe, there is an inherent "modulo-d ambiguity" and therefore we cannot *a priori* assign a particular value to n. The experimentally determined P_{004} values indicate that the ordered Ba and Sr atoms are located at respective heights of $(1.34 + nd_{004})$ Å and $(1.20 + nd_{004})$ Å above the ideal bulk height of second layer Si atoms. The 0.14 Å height difference between the AEM adatoms in the two different types of surface phases is similar to the 0.16–0.17 Å difference between the Ba^{2+} and Sr^{2+} ionic radii.[39]

In a previous XSW study of a two-domain (2×3) Sr/Si(001) surface[24] with a coverage of 0.12(3) ML,

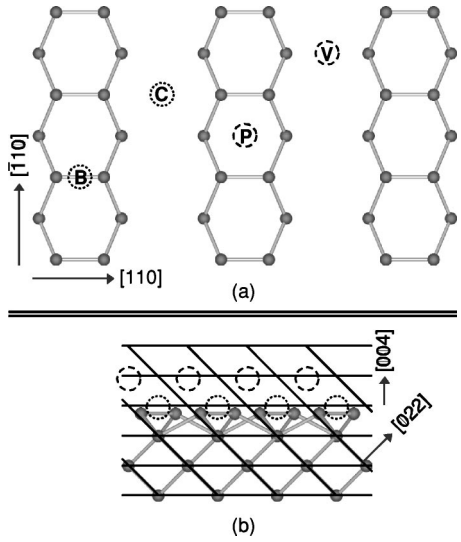

FIG. 2. (a) [001] projection of dimerized Si(001) surface. If $n=0$ in Eq. (1), then the AEM adsorption sites would be restricted to the bridge (B) and cave (C) high-symmetry sites. If $n=1$, then the AEM adsorption sites would be limited to the pedestal (P) and valley-bridge high-symmetry sites. (b) [100] projection showing the out-of-plane positions of AEM atoms if $n=0$ (dotted circles) and $n=1$ (dashed circles). Horizontal and 45° tilted solid lines represent Si(004) and Si(022) diffraction planes, respectively.

we reported the following Sr coherent positions and fractions: $P_{004}=0.86(1)$, $f_{004}=0.56(2)$, $P_{022}=0.42(1)$, and $f_{022}=0.59(4)$. The differences between the Sr coherent positions measured for the (2×3) and (2×1) phases [see Figs. 1(b) and 1(c)] are only marginally larger than the experimental error, but they do suggest that the Sr height in the (2×3) phase is slightly lower than that in the (2×1) phase. The fact that $P_{022}\approx P_{004}/2$ for both the (2×1) and (2×3) Sr/Si(001) phases as well as the (2×1) Ba/Si(001) phase provides strong evidence that the ordered fraction of adatoms occupies the same type of in-plane site in all three of these AEM/Si(001) surface phases.

Most models that have been proposed previously for Ba/Si(001) and Sr/Si(001) surfaces consist of AEM adatoms sitting on a dimerized top layer of Si atoms. Some experimental evidence does seem to support the presence of top layer Si dimers in these AEM/Si(001) surface phases. An XPS of study[22] of the (2×3) and (2×1) Sr/Si(001) surfaces has suggested that the top layer Si atoms remain dimerized in both of these surface phases and that unlike the buckled Si dimers found on the clean Si(001)-(2×1) reconstructed surface, those in the (2×3) and (2×1) Sr/Si(001) surfaces are symmetric. Several DFT calculations of Ba/Si(001) and Sr/Si(001) surfaces have indicated that the top layer Si dimers remain for AEM coverage up to at least 1/2 ML, and Ciani *et al.*[25] found that Si dimerization is still energetically favorable (by 0.2 eV per dimer) at 1 ML Ba coverage.

A symmetrically dimerized Si(001) surface contains four high symmetry sites: the bridge, cave, pedestal, and valley-bridge sites shown in Fig. 2(a). If it is assumed that the ordered AEM atoms occupy only one type of site (and that this site is a high symmetry site), the AEM adatom position relative to the bulk primitive unit cell of the Si lattice can be uniquely determined in three dimensions using less than three P_H values. The assumption that AEM atoms order onto a single, high-symmetry site is supported by the fact that $f_{004}\approx f_{022}$ for both Ba and Sr. In our investigation of the 1/6 ML (2×3) Sr/Si(001) surface,[24] results of XSW measurements made along a third (hkl) direction, (111), provided further evidence that the (2×3) unit cell consists of Sr atoms occupying only one type of site.

TABLE I. Nearest neighbor AEM-Si distances that would result from Ba and Sr adsorption at high-symmetry sites on the dimerized Si(001) surface (at the bulk primitive Si unit cell positions determined by XSW).

Adatom	Adsorption site	Nearest neighbor AEM-Si distance (Å)
Ba	bridge	1.16
Ba	cave	2.74
Ba	pedestal	2.78
Ba	valley-bridge	3.31
Sr	bridge	1.13
Sr	cave	2.73
Sr	pedestal	2.70
Sr	valley-bridge	3.20

If $n=0$ in Eq. (1), then the experimentally determined P_{004} and P_{022} values would be consistent with AEM atoms occupying cave or bridge sites on a dimerized Si(001) surface. If $n=1$ in Eq. (1), our P_{004} and P_{022} values would restrict the in-plane position of ordered AEM atoms to valley-bridge or pedestal sites. The out-of-plane positions of AEM atoms for both $n=0$ and $n=1$ are shown in the [100] side-view projection of Fig. 2(b). XSW results alone cannot distinguish between these four high symmetry positions because they all represent the same position within the bulk primitive Si unit cell. Each of these sites still represents a unique position within the surface unit cell, and AEM occupation of any one of these sites would result in a distinct set of AEM-Si bond lengths.

Table I shows the nearest neighbor AEM-Si bond lengths that would result from Ba and Sr atoms occupying each of these high symmetry sites at the heights determined from the Ba and Sr coherent positions. The top-layer Si atomic positions given by Roberts' model for a symmetrically dimerized Si(001)-(2×1) surface[40] are used when calculating the AEM-Si bond lengths (and when drawing Fig. 2) in order to approximate the presumably symmetric structure[22,26] of Si dimers in the AEM/Si(001) surface reconstructions. Since no accommodation was made for the relaxation of Si atoms away from these assumed positions when calculating the bond lengths listed in Table I, these values should only be considered accurate to within 0.2 Å (DFT calculations[25] have predicted that the presence of AEM atoms on Si(001) would cause an increase in the height of top layer Si dimers, and the magnitude of this height change was found to depend on both the in-plane position and total coverage of the AEM atoms). The bridge site on dimerized Si(001) can immedi-

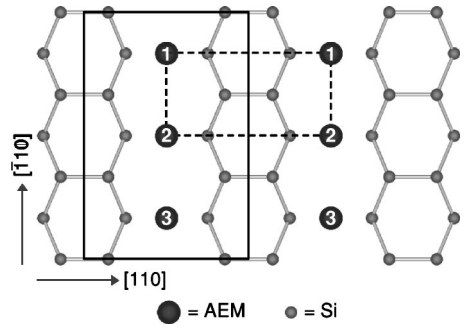

FIG. 3. Top-view [001] projection showing AEM atoms at valley-bridge sites. Outlines of (2×1) (dashed line) and (2×3) (solid line) unit cells are also drawn. All AEM atoms labeled "1," "2," and "3" would be present in the (2×1) phase. (2×3) periodicity would arise from the removal of AEM atoms labeled 2 and/or 3.

ately be ruled out as a possible AEM adsorption site due to steric hindrance. The nearest neighbor AEM-Si bond lengths for Ba and Sr atoms occupying this site would be more than 50% shorter than the 3.2–3.5 Å Ba—Si (Ref. 41) and 3.2–3.4 Å Sr—Si (Ref. 42) nearest neighbor distances found in bulk AEM-Si compounds. The nearest neighbor Ba-Si and Sr-Si bond lengths for AEM atoms located at cave and pedestal sites would be greater than those expected for bridge site adsorption, but would still be 0.5–0.8 Å shorter than bulk AEM-Si nearest neighbor distances. Ba and Sr adsorption at valley-bridge sites, however, would result in AEM-Si nearest neighbor bond lengths that fall within the range of nearest neighbor distances observed in bulk compounds. These bond length considerations suggest that if the top layer Si atoms do remain dimerized in the (2×1) Ba/Si(001) and Sr/Si(001) surfaces, then the valley-bridge site is the most plausible AEM atom adsorption site in these surface phases.

The top-view [001] projection of the (2×1) AEM/Si(001) surface model in Fig. 3 shows AEM atoms occupying all of the valley-bridge sites—i.e., at a coverage of 1/2 ML. Since every (2×1) unit cell of an AEM/Si(001) surface phase must contain at least one AEM atom, and the areal number density of surface unit cells on any (2×1) reconstructed Si(001) surface is 1/2 ML, the AEM saturation coverage of a (2×1) AEM/Si(001) surface phase must be *at least* 1/2 ML. The total coverages (0.3–0.6 ML) we have measured for (2×1) surfaces seem to be consistent with a 1/2 ML saturation coverage. It is important to note that the AEM coherent coverage, θ_C, given by

$$\theta_C = f_H \theta_T \tag{2}$$

where θ_T is the total coverage, was only 0.13 ML for Ba and 0.15 ML for Sr on the (2×1) surfaces for which XSW data is shown in Fig. 1. The differences between the θ_T and θ_C coverage values, and the fact that (2×1) AEM/Si(001) surface phases have been observed at θ_T below 1/2 ML, demonstrate the coexistence of regions of 1/2 ML (2×1) AEM/Si(001) surface phase with disordered AEM atoms and regions where the local AEM coverage is below 1/2 ML. It is likely that the relative amounts of (2×1) ordered AEM atoms, disordered AEM atoms and regions with a local coverage below 1/2 ML are highly dependent on sample preparation conditions. The potential for such variation could explain why McKee *et al.*[43,44] observed a 1/4 ML saturation coverage for (2×1) phases of both Ba and Sr on Si(001).

Figure 3 also shows the (2×3) AEM/Si(001) unit cells that would result from AEM atoms occupying 1/3 or 2/3 of the valley-bridge sites (at respective local coverages of 1/6 and 1/3 ML). Note that when discussing our XSW results for the (2×3) Sr/Si(001) surface in Ref. 24, only the case of $n=0$ (and not $n=1$) was considered in Eq. (1), and it was proposed that Sr atoms occupy cave sites in a 1/6 ML (2×3) phase. This conclusion was similar to Bakhtizin *et al.*'s[14] proposal that a 1/3 ML (2×3) Sr/Si(001) surface consisted of Sr occupying 2/3 of the cave sites, and Kim *et al.*'s[20] suggestion that Ba atoms occupy cave sites in 1/6 ML (2×3) and 1/2 ML (2×1) Ba/Si(001) surface phases. Based on the AEM-Si bond length considerations described earlier, along with mounting evidence from DFT calculations, it now appears that the valley-bridge site may be the most plausible Sr adsorption site in the 1/6 ML (2×3) Sr/Si(001) surface phase.

Herrera-Gómez *et al.*[23] previously studied the (2×1) Ba/Si(001) surface with XSW using two off-normal Si {111} reflections. Ba adatoms located at the bulk-primitive unit cell position indicated by our (004) and (022) XSW measurements would be expected to yield $P_{\{111\}}=0.75$ [with the (111) planes drawn through the middle of the Si bilayers and assuming equal population of both orientations of (2×1) surface domains]. Herrera-Gómez *et al.* measured $P_{1\bar{1}1}=0.75$ and $P_{\bar{1}\bar{1}1}=0.70$. The difference between these two coherent positions was assumed to be due the presence of unequal amounts of the two orientations of (2×1) domains, and it was concluded that Ba atoms sit in valley-bridge sites at a height 2.58 Å above the ideal bulk plane of second layer Si atoms (our data indicates that Ba atoms occupying valley-bridge sites would sit 2.70 Å above the bulk plane of second layer Si atoms).

DFT calculations have in fact indicated that the valley-bridge site is the minimum energy adsorption site for isolated Ba and Sr atoms on dimerized Si(001) and that AEM atoms are expected to occupy this same site to form a 1/2 ML (2×1) phase.[5,25,26,28] Other studies have also supported the idea that, at least for room-temperature AEM adsorption onto Si(001), the top layer Si atoms remain dimerized, and the valley-bridge site is the minimum energy adsorption site. STM studies of the initial stages (up to 0.06 ML) of Ba adsorption onto room-temperature Si(001) showed most of the Ba adatoms occupying valley-bridge sites.[17,18] An ion-scattering study of Ba adsorbed onto room-temperature Si(001) also concluded that Ba preferentially occupied valley-bridge sites at a height of 3.00 ± 0.05 Å above the second layer Si(001) plane.[21]

The 0.30 Å difference between this height and that specified by our XSW measurements for valley-bridge site occupancy could be due to experimental errors in the ion scattering and/or XSW measurements. The difference between the two measurements could also be due to the fact that XSW

determines the adatom position relative to the bulk position of Si lattice planes, while ion scattering should be sensitive to the distance between adatoms and the actual Si atomic positions. Relaxation of the second layer Si atoms away from their bulk positions would therefore cause the XSW and ion scattering techniques to measure different heights. However, the vertical relaxation distances of second layer Si atoms are expected to be less than 0.10 Å (Ref. 25) and most likely would not account for the entire difference between the heights indicated by the two techniques. It is also possible that the discrepancy between the XSW and ion-scattering results is due to actual differences between the heights of room-temperature adsorbed Ba (studied by ion scattering) and Ba atoms in the long-range ordered surface phases (studied by XSW) formed at elevated temperatures.

Although such a height difference would not necessarily indicate a difference in in-plane Ba positions, some experimental evidence does suggest that the (2×3) and (2×1) AEM/Si(001) surface phases formed at high temperatures consist of AEM atoms occupying a site other than the valley-bridge site. As mentioned earlier, STM images have clearly identified Ba atoms adsorbed at valley-bridge sites and have also shown how valley-bridge adsorbed Ba can form chains that "zig-zag" across Si dimer rows.[17–19] However, both filled and empty state STM images of Ba/Si(001) have shown that the local density of states of (2×3) Ba/Si(001) surfaces is markedly different from that of surface regions where Ba is adsorbed at valley-bridge sites.[16,19] This difference is particularly apparent when regions of (2×3) phase are shown coexisting with other regions containing Ba adsorbed at valley-bridge sites in the same image (see Fig. 2 of Ref. 19). Similarly, STM images of (2×3) and (2×1) Sr/Si(001) surfaces formed at 700–800 °C indicated that the local atomic-scale structure of these surface phases differed significantly from that of the zig-zag chains (presumably consisting of Sr atoms at valley-bridge sites) that formed upon deposition of Sr onto room-temperature Si(001).[14,45]

Based on their STM images, Hu *et al.*[19] have made a compelling argument that formation of the (2×3) Ba/Si(001) surface involves the removal of dimerized top layer Si atoms and that individual Ba atoms end up occupying 1/3 or 2/3 of the sites formerly occupied by Si dimers. In other STM studies, Ojima *et al.* also suggested that the (2×3) Ba/Si(001) surface[16] as well as a wavy "1×2" surface[15] formed via the removal of Si dimers. In these cases, however, it was proposed that a portion of the former Si dimer sites were always occupied by Ba dimers (rather than individual Ba atoms). Our XSW results would be consistent with individual AEM atoms substituting for Si dimers. In this atomic arrangement, AEM adatoms would essentially be occupying bridge sites, but the removal of top layer Si dimers would eliminate the steric hindrance effects that make bridge site occupancy improbable on a dimerized Si(001) surface. Any atomic-scale structural model lacking Si dimers would however, seem to contradict XPS findings that Si dimer states remain in the (2×3) and (2×1) Sr/Si(001) surface phases.[22]

The nearest neighbor AEM-Si bond lengths that would result from Ba and Sr occupying high symmetry sites at the heights consistent with our XSW data (see Table I) suggest that if AEM adatoms in the (2×3) and (2×1) surfaces do not occupy valley-bridge sites, but the top layer Si atoms still remain dimerized, either the cave or pedestal site would be the most plausible in-plane adatom position (AEM occupancy of either of these sites would result in AEM-Si bond lengths 0.5–0.8 Å shorter than bulk AEM-Si bond lengths, while the bond lengths resulting from bridge site occupancy would be 2.1–2.3 Å shorter than bulk AEM-Si bond lengths). The slight differences ($\leqslant$0.08 Å) among the AEM-Si bond lengths calculated for cave and pedestal site occupancy are insignificant relative to the error expected from assuming that the Si atoms remain fixed at the positions shown in Fig. 2. However, DFT calculations have indicated that the pedestal site is the second most energetically favorable AEM adsorption site (behind the valley-bridge site).[25–27]

IV. CONCLUSIONS

XSW measurements have been used to study submonolayer phases of Ba and Sr on the Si(001) surface and have determined the AEM atom positions relative to the bulk primitive Si unit cell. Our results indicate that the Ba and Sr atoms are located in the same type of site in the (2×1) Ba/Si(001), (2×1) Sr/Si(001), and (2×3) Sr/Si(001) surface phases. Adatoms in the (2×1) Ba/Si(001) phase are found to sit 0.14 Å higher than those in the (2×1) Sr/Si(001) phase. The experimentally measured (004) and (022) coherent positions are consistent with the AEM atoms occupying cave or bridge sites (at a height similar to that of the top layer Si atoms), or pedestal or valley-bridge sites [at a height one Si(004) *d* spacing higher than the proposed cave / bridge site heights]. A comparison of the nearest neighbor AEM-Si bond lengths that would result from AEM atoms located at these positions strongly suggests that AEM atoms occupy valley-bridge sites (in agreement with DFT predictions).

ACKNOWLEDGMENTS

The authors gratefully acknowledge the BESSRC-CAT staff at the Argonne National Laboratory Advanced Photon Source for assistance with XSW experiments, and also thank L. Funk and P. Baldo of MSD/ANL for providing the RBS calibrated implanted standards used for coverage determination. This work was supported by NSF under Contract Nos. DMR-0076097 and DMR-9973436, and by the DOE under Contract Nos. W-31-109-Eng-38 and DE-FG02-03ER15457.

[1] Y. Wang, C. Ganpule, B. T. Liu, H. Li, K. Mori, B. Hill, M. Wuttig, R. Ramesh, J. Finder, Z. Yu, R. Droopad, and K. Eisenbeiser, Appl. Phys. Lett. **80**, 97 (2002).
[2] B. T. Liu, K. Maki, Y. So, V. Nagarajan, R. Ramesh, J. Lettieri, J. H. Haeni, D. G. Schlom, W. Tian, X. Q. Pan, F. J. Walker, and R. A. McKee, Appl. Phys. Lett. **80**, 4801 (2002).
[3] R. A. McKee, F. J. Walker, and M. F. Chisholm, Phys. Rev. Lett. **81**, 3014 (1998).
[4] H. Li, X. Hu, Y. Wei, Z. Yu, X. Zhang, R. Droopad, A. A. Demkov, J. Edwards, K. Moore, W. Ooms, J. Kulik, and P. Fejes, J. Appl. Phys. **93**, 4521 (2003).
[5] R. Droopad, Z. Yu, J. Ramdani, L. Hilt, J. Curless, C. Overgaard, J. L. Edwards, J. Finder, K. Eisenbeiser, J. Wang, V. Kaushik, B.-Y. Ngyuen, and B. Ooms, J. Cryst. Growth **227–228**, 936 (2001).
[6] W. C. Fan, N. J. Wu, and A. Ignatiev, Phys. Rev. B **42**, 1254 (1990).
[7] W. C. Fan and A. Ignatiev, Surf. Sci. **253**, 297 (1991).
[8] D. Vlachos, M. Kamaratos, and C. Papageorgopoulos, Solid State Commun. **90**, 175 (1994).
[9] T. Urano, K. Tamiya, K. Ojima, S. Hongo, and T. Kanaji, Surf. Sci. **358**, 459 (1996).
[10] Y. Takeda, T. Urano, T. Ohtani, K. Tamiya, and S. Hongo, Surf. Sci. **404**, 692 (1998).
[11] X. Hu, C. A. Peterson, D. Sarid, Z. Yu, J. Wang, D. S. Marshall, R. Droopad, J. A. Hallmark, and W. J. Ooms, Surf. Sci. **426**, 69 (1999).
[12] X. Hu, Z. Yu, J. A. Curless, R. Droopad, K. Eisenbeiser, J. L. Edwards, Jr., W. J. Ooms, and D. Sarid, Appl. Surf. Sci. **181**, 103 (2001).
[13] J. Lettieri, J. H. Haeni, and D. G. Schlom, J. Vac. Sci. Technol. A **20**, 1332 (2002).
[14] R. Z. Bakhtizin, J. Kishimoto, T. Hashizume, and T. Sakurai, Appl. Surf. Sci. **94–95**, 478 (1996); R. Z. Bakhtizin, J. Kishimoto, T. Hashizume, and T. Sakurai, J. Vac. Sci. Technol. B **14**, 1000 (1996).
[15] K. Ojima, M. Yoshimura, and K. Ueda, Phys. Rev. B **65**, 075408 (2002).
[16] K. Ojima, M. Yoshimura, and K. Ueda, Surf. Sci. **491**, 169 (2001).
[17] X. Yao, X. M. Hu, D. Sarid, Z. Yu, J. Wang, D. S. Marshall, R. Droopad, J. K. Abrokwah, J. A. Hallmark, and W. J. Ooms, Phys. Rev. B **59**, 5115 (1999).
[18] X. Hu, X. Yao, C. A. Peterson, D. Sarid, Z. Yu, J. Wang, D. S. Marshall, J. A. Curless, J. Ramdani, R. Droopad, J. A. Hallmark, and W. J. Ooms, Surf. Sci. **457**, L391 (2000).
[19] X. Hu, X. Yao, C. A. Peterson, D. Sarid, Z. Yu, J. Wang, D. S. Marshall, R. Droopad, J. A. Hallmark, and W. J. Ooms, Surf. Sci. **445**, 256 (2000).
[20] J. S. Kim, K. W. Ihm, C. C. Hwang, H. S. Kim, Y. K. Kim, C. G. Lee, and C. Y. Park, Jpn. J. Appl. Phys., Part 1 **38**, 6479 (1999).
[21] W. S. Cho, J. Y. Kim, S. S. Kim, D. S. Choi, K. Jeong, I. W. Lyo, C. N. Whang, and K. H. Chae, Surf. Sci. **476**, L259 (2001).
[22] A. Herrera-Gómez, F. S. Aguirre-Tostado, Y. Sun, P. Pianetta, Z. Yu, D. Marshall, R. Droopad, and W. E. Spicer, J. Appl. Phys. **90**, 6070 (2001).
[23] A. Herrera-Gomez, P. Pianetta, D. Marshall, E. Nelson, and W. E. Spicer, Phys. Rev. B **61**, 12 988 (2000).
[24] D. M. Goodner, D. L. Marasco, A. A. Escuadro, L. Cao, B. P. Tinkham, and M. J. Bedzyk, Surf. Sci. **547**, 19 (2003).
[25] A. J. Ciani, P. Sen, and I. P. Batra, Phys. Rev. B **69**, 245308 (2004).
[26] C. R. Ashman, C. J. Forst, K. Schwarz, and P. E. Blochl, Phys. Rev. B **69**, 075309 (2004).
[27] J. Wang, J. A. Hallmark, D. S. Marshall, W. J. Ooms, P. Ordejon, J. Junquera, D. Sanchez-Portal, E. Artacho, and J. M. Soler, Phys. Rev. B **60**, 4968 (1999).
[28] R. Droopad, Z. Y. Yu, H. Li, Y. Liang, C. Overgaard, A. Demkov, X. D. Zhang, K. Moore, K. Eisenbeiser, M. Hu, J. Curless, and J. Finder, J. Cryst. Growth **251**, 638 (2003).
[29] X. M. Hu, H. Li, Y. Liang, Y. Wei, Z. Yu, D. Marshall, J. Edwards, R. Droopad, X. Zhang, A. A. Demkov, K. Moore, and J. Kulik, Appl. Phys. Lett. **82**, 203 (2003).
[30] C. J. Forst, C. R. Ashman, K. Schwarz, and P. E. Blochl, Nature (London) **427**, 53 (2004).
[31] F. S. Aguirre-Tostado, A. Herrera-Gomez, J. C. Woicik, R. Droopad, Z. Yu, D. G. Schlom, J. Karapetrova, P. Zschack, and P. Pianetta, J. Vac. Sci. Technol. A **22**, 1356 (2004).
[32] F. S. Aguirre-Tostado, A. Herrera-Gomez, J. C. Woicik, R. Droopad, Z. Yu, D. G. Schlom, P. Zschack, E. Karapetrova, P. Pianetta, and C. S. Hellberg, Phys. Rev. B **70**, 201403(R) (2004).
[33] S. A. Chambers, T. Droubay, T. C. Kaspar, and M. Gutowski, J. Vac. Sci. Technol. B **22**, 2205 (2004).
[34] F. Amy, A. S. Wan, A. Kahn, F. J. Walker, and R. A. McKee, J. Appl. Phys. **96**, 1601 (2004); **96**, 1635 (2004).
[35] Y. Wei, X. M. Hu, Y. Liang, D. C. Jordan, B. Craigo, R. Droopad, Z. Yu, A. Demkov, J. L. Edwards, and W. J. Ooms, J. Vac. Sci. Technol. B **20**, 1402 (2002).
[36] A. Ishizaka and Y. Shiraki, J. Electrochem. Soc. **133**, 666 (1986).
[37] J. Zegenhagen, Surf. Sci. Rep. **18**, 199 (1993).
[38] M. J. Bedzyk and L. W. Cheng, Rev. Mineral. Geochem. **49**, 221 (2002).
[39] F. A. Cotton, G. Wilkinson, C. A. Murillo, and M. Bochman, *Advanced Inorganic Chemistry* (Wiley, New York, 1999).
[40] N. Roberts and R. J. Needs, Surf. Sci. **236**, 112 (1990).
[41] H. Schafer, K. Janzon, and A. Weib, Angew. Chem., Int. Ed. Engl. **2**, 393 (1963); K. Janzon, H. Schafer, and A. Weiss, Z. Naturforsch. B **21**, 287 (1966); B. Eisenman, K. Janzon, H. Schafer, and A. Weiss, *ibid.* **24**, 457 (1969); A. Widera and H. Schafer, *ibid.* **31**, 1434 (1976); G. Bruzzone and E. Franceschi, J. Less-Common Met. **57**, 201 (1978).
[42] G. Rocktaschel and A. Weiss, Z. Anorg. Allg. Chem. **316**, 231 (1962); K. Janzon, H. Schafer, and A. Weiss, Angew. Chem., Int. Ed. Engl. **4**, 245 (1965); G. Nagorsen, G. Rocktaschel, H. Schafer, and A. Weiss, Z. Naturforsch. B **22**, 101 (1967); A. Widera, B. Eisenmann, and H. Schafer, *ibid.* **31**, 520 (1976); J. Evers, G. Oehlinger, and A. Weiss, *ibid.* **38**, 899 (1983); G. E. Pringle, Acta Crystallogr., Sect. B: Struct. Crystallogr. Cryst. Chem. **28**, 2326 (1972); J. Evers, G. Oehlinger, and A. Weiss, J. Solid State Chem. **20**, 173 (1977); G. Bruzzone and E. Franceschi, J. Less-Common Met. **57**, 201 (1978).
[43] R. A. McKee, F. J. Walker, J. R. Conner, and R. Raj, Appl. Phys. Lett. **63**, 2818 (1993).
[44] R. A. McKee, F. J. Walker, M. B. Nardelli, W. A. Shelton, and G. M. Stocks, Science **300**, 1726 (2003).
[45] Z. Yu, Y. Liang, C. Overgaard, X. Hu, J. Curless, H. Li, Y. Wei, B. Craigo, D. Jordan, R. Droopad, J. Finder, K. Eisenbeiser, D. Marshall, K. Moore, J. Kulik, and P. Fejes, Thin Solid Films **462-63**, 51 (2004).